Water Research 247 (2023) 120842

Contents lists available at ScienceDirect

Water Research

journal homepage: www.elsevier.com/locate/watres

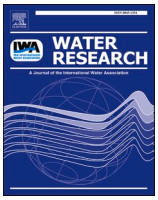

Estimation of ecosystem respiration and photosynthesis in supersaturated stream water downstream of a hydropower plant

Benoît O.L. Demars [a,*], Peter Dörsch [b]

[a] Norwegian Institute for Water Research (NIVA), Økernveien 94, Oslo 0579, Norway
[b] Faculty of Environmental Sciences and Natural Resource Management, Norwegian University of Life Sciences, Ås 1432, Norway

ARTICLE INFO

Keywords:
Whole stream metabolism
Noble gas
Argon
Gas exchange
Aquatic plant
Light use efficiency

ABSTRACT

The estimation of whole stream metabolism, as determined by photosynthesis and respiration, is critical to our understanding of carbon cycling and carbon subsidies to aquatic food-webs. The mass development of aquatic plants is a worldwide problem for human activities and often occurs in regulated rivers, altering biodiversity and ecosystem functions. Hydropower plants supersaturate water with gases and prevent the use of common whole stream metabolism models to estimate ecosystem respiration. Here we used the inert noble gas argon to parse out biological from physical processes in stream metabolism calculations. We coupled the O_2:Ar ratio determined by gas chromatography in grab samples with *in-situ* oxygen concentrations measured by an optode to estimate aquatic plant photosynthesis and ecosystem respiration during supersaturation events through a parsimonious approach. The results compared well with a more complicated two-station model based on O_2 mass balances in non-supersatured water, and with associated changes in dissolved CO_2 (or dissolved inorganic carbon). This new method provides an independent approach to evaluate alternative corrections of dissolved oxygen data (e.g. through the use of total dissolved gases) in long term studies. The use of photosynthesis-irradiance models allows the determination of light parameters such as the onset of light saturation or low light use efficiency, which could be used for inverse modelling. The use of the O_2:Ar approach to correct for oversaturation may become more applicable with the emergence of portable mass inlet mass spectrometers (MIMS). Photosynthesis was modest (2.9-5.8 g O_2 m^2 day^{-1}) compared to other rivers with submerged vegetation, likely indicating nutrient co-limitations (CO_2, inorganic N and P). Respiration was very low (-2.1 to -3.9 g O_2 m^2 day^{-1}) likely due to a lack of allochthonous carbon supply and sandy sediment.

1. Introduction

The estimation of whole stream metabolism, as determined by photosynthesis and respiration, is critical to our understanding of carbon cycling and carbon subsidies to aquatic food-webs. Rivers contribute net emissions of CO_2 and CH_4 of the same order of magnitude as terrestrial carbon sequestration (Battin et al. 2023, Dawson 2013, Rocher-Ros et al. 2023). The metabolic balance of streams (photosynthesis – respiration) allows to estimate the degradation of land derived organic carbon in fluvial systems (Demars 2019, Hall et al. 2016, Hotchkiss et al. 2015) but remains poorly constrained at the global scale (Battin et al. 2023). Stream metabolism quantifies river productivity, notably the relative importance of autotrophs and heterotrophs to the flow of carbon through the base of food webs (Cross et al. 2013, Demars et al. 2020, Marcarelli et al. 2011, O'Gorman et al. 2016).

The open-channel diel oxygen method to quantify stream metabolism (Odum 1956) has been applied across the world and at continental scale (Appling et al. 2018b, Bernhardt et al. 2022, Demars et al. 2016). The method quantifies the *in-situ* (open-channel) rate of change in dissolved oxygen mass with respect to time as a function of aerobic respiration, photosynthesis and gas exchange fluxes at the air-water interface. Corrections for lateral inflows may also be necessary (McCutchan et al. 2002). While the first principles are simple, spatial heterogeneity and temporal variability can make applications in rivers challenging (Demars et al. 2015). The method may be applied with data from one station (area of stream defined from the dissolved oxygen sensor footprint, a function of velocity and gas exchange rate) or two stations (reach area defined by the top and bottom stations). Whether or how the two-station method may remove the effects of upstream discontinuity is still an open debate (Demars et al. 2015). New methods

* Correspoding author.
E-mail address: benoit.demars@niva.no (B.O.L. Demars).

https://doi.org/10.1016/j.watres.2023.120842
Received 23 July 2023; Received in revised form 1 November 2023; Accepted 5 November 2023
Available online 6 November 2023

strive to improve the quantification of stream metabolism and its uncertainties in space and time: inverse models with maximum likelihood or Bayesian statistics (e.g. Appling et al. 2018a, Grace et al. 2015), the use of oxygen stable isotope ratios ($\delta^{18}O$–O_2, Holtgrieve et al. 2010, Hotchkiss and Hall 2014, Tromboni et al. 2022), accounting method with Monte Carlo simulations (Demars 2019).

The mass development of submersed macrophytes is a worldwide problem and often seen as nuisance for human activities (Thiemer et al. 2023, Verhofstad and Bakker 2019). Undesirable plant growth leads to costly remedial actions with variable effectiveness (Hussner et al. 2017, Rørslett and Johansen 1996) and alters aquatic biodiversity and ecosystem functioning (Schultz and Dibble 2012, Thiemer et al. 2021, Velle et al. 2022). River regulation and associated geomorphological changes support the development of large stands of aquatic macrophytes by removing natural hydrological peaks and changing them to diel hydropeaking (Gurnell 2014, Rørslett 1988, Rørslett et al. 1989). Mechanical harvesting is often used to remove aquatic plants. Knowledge of macrophyte growth and its main drivers could help to support remedial management decisions (Thiemer et al. 2021).

Many rivers of the world are highly fragmented and flow regulated (Grill et al. 2019, Nilsson et al. 2005). This creates a need for more advanced approaches including flow routing models with two-station metabolism models (e.g. Pathak and Demars 2023, Payn et al. 2017). However, current models can only estimate photosynthesis and not respiration in river sections with gas supersaturation downstream of hydropower plants, thermal discharge or white-water rapids (e.g. Demars et al. 2023, Hall Jr et al. 2012, Hall et al. 2015), unless additional corrections on dissolved oxygen concentrations are introduced, e.g. through the use of total dissolved gas time series (Roley et al. 2023).

The reasons are to do with gas exchange processes. Atmospheric gas exchange depends on molecular diffusion through unbroken water surfaces. In addition, bubble-mediated mass flow must be considered for broken water surfaces (e.g. Asher and Wanninkhof 1998, Emerson et al. 1991, Howard et al. 2010), such as downstream cascades, engineering structures and turbulent small streams (e.g. Demars and Manson 2013, Ulseth et al. 2019). Theoretical models for gas exchange rates derived from first principles are helpful to understand specific mechanisms, such as temperature dependency of gas exchange or behaviour of multiple gases with different diffusion velocities and solubilities (e.g. Demars and Manson 2013, Hall and Madinger 2018). However, the direct application of theoretical models to field studies remains challenging (e.g. Schierholz et al. 2006, Urban and Gulliver 2000). Thus, the gas exchange is generally derived empirically from gas tracer studies, floating flux chambers or oxygen diel changes (Demars et al. 2015, Holtgrieve et al. 2016), which, however, cannot separate the role of biologically and physically driven gas fluxes.

One solution to partition biological from physical processes is the use of natural inert tracers with diffusion and solubility properties similar to oxygen. The O_2:Ar ratio method has been used previously to parse out physical from biological processes in marine studies (e.g. Craig and Hayward 1987, Emerson et al. 1991, Howard et al. 2010), lakes (e.g. Craig et al. 1992, Wilkinson et al. 2015), an estuary (Manning et al. 2019) and the hyporheic zone of a river (Machler et al. 2013). Here we combine the O_2:Ar ratio with *in-situ* oxygen optode measurements to estimate stream metabolism (both photosynthesis and respiration) in a river with known total dissolved gas supersaturation from a hydropower plant and aquatic plant mass development (Pulg et al. 2022, Pulg et al. 2016a, Stenberg et al. 2022). We also investigated the concomitant changes in dissolved CO_2 concentrations and discussed their potential role in limiting aquatic plant photosynthesis.

2. Theory

A simple equation describing the change in mass of oxygen (dm) relative to change in time (dt) over a parcel of water moving downstream, and excluding lateral inflows, is (Odum 1956):

$$\frac{dm}{dt} = (metabolism + atmospheric\ gas\ exchange\ flux) \times wetted\ area \quad (1)$$

$$\frac{dm}{dt} = [(GPP - ER) + K_L(C_s - C_t)] \quad (2)$$

where m is mass of oxygen (g O_2), t time (hour), GPP gross primary production, ER ecosystem respiration (g O_2 m^{-2} $hour^{-1}$), K_L gas exchange velocity (m $hour^{-1}$), A area of surface water (m^2), C_s concentration of oxygen at atmospheric saturation (g O_2 m^{-3}) and C_t the concentration of oxygen at time t (g O_2 m^{-3}).

This can be reformulated as change in dissolved oxygen concentration (C) by dividing by the volume of the parcel of water and introducing $GPP_t - ER_t = NEP_t$, net ecosystem production (g O_2 m^{-2} $hour^{-1}$):

$$\frac{dC}{dt} = \frac{NEP_t + K_L(C_s - C_t)}{z} \quad (3)$$

with z, average stream water depth.

The net metabolism of an aquatic ecosystem can then be computed from a single diel oxygen curve, the gas transfer velocity, and the mixing depth (Odum 1956). The change in O_2 concentration at a single station between two subsequent measurements can be approximated as:

$$\frac{dC}{dt} = \frac{C_t - C_{t-\Delta t}}{\Delta t} \quad (4)$$

After combining the latter two equations and with $k = K_L/z$ gas exchange coefficient ($hour^{-1}$) and rearranging terms for an accounting (book-keeping) approach, we obtain

$$NEP_t = \left(\frac{C_t - C_{t-\Delta t}}{\Delta t} - k(C_s - C_t)\right) z \quad (5)$$

This simple model assumes that all changes in oxygen as well as the saturation deficit are due to biological processes. This assumption does not apply where gas supersaturation occurs due to physical processes, such as downstream of natural cascades, white water or engineering structures (e.g. hydropower plants).

In most studies, the gas exchange velocity K_L is derived from a model parameterized as the sum of diffusive exchange and mass flow (bubble processes) – (e.g. Emerson et al. 1991, Howard et al. 2010). For argon, an equation similar to the oxygen mass balance is written but without the biological production term, and NEP is derived from these two equations assuming argon and oxygen have identical diffusivities and solubilities (e.g. Emerson et al. 1991, Howard et al. 2010). The O_2-Ar supersaturation difference, ΔO_2 – ΔAr (with ΔO_2=C-C_s and ΔAr=C_{Ar}-$C_{Ar,s}$) is commonly approximated as $\Delta O_2/Ar$ but NEP may be biased when Ar concentration deviates substantially from saturation at equilibrium (Eveleth et al. 2014).

Here, we propose a simpler and unbiased approach to estimate stream metabolism in supersaturated water from diel O_2 fluctuations. We adjust the GC-measured O_2 molar concentrations by using the measured O_2:Ar ratio to estimate *in-situ* Ar molar concentrations from *in-situ* O_2 optode measurements, which then can be used to correct for physical processes leading to gas under- or over-saturation. As a by-product, we remove analytical noise in oxygen molar concentrations originating from the GC-headspace method (assuming that errors in O_2 and Ar measured by GC are proportional, Eq. 7):

$$C = \frac{C_{GC,O_2}}{C_{GC,Ar}} \overline{C_{Ar}} \Big/ \overline{E_{pAr}} \quad (6)$$

with $\overline{C_{Ar}}$ *in-situ* daily averaged molar concentration of argon, a latent variable, calculated from individual datapoints as in Eveleth et al. (2014) as follows:

$$C_{Ar} = \frac{C_{optode,O_2}}{C_{GC,O_2}} C_{GC,Ar} \quad (7)$$

with C_{optode,O_2} being the oxygen molar concentration from an *in-situ* optode. We also have:

$$E_{pAr} = \frac{C_{Ar}}{C_{Ar,expected}} \quad (8)$$

with E_{pAr} the excess partial pressure of argon (E*p*Ar) and $C_{Ar,expected}$ the molar concentration of argon expected at observed water temperature and atmospheric pressure. In Eq. (6), $\overline{E_{pAr}}$ is the *in-situ* daily averaged E*p*Ar. The first term on the right-hand side of Eq. (6) essentially corrects the amplitude of the *in-situ* optode O_2 molar concentration, the second term adjusts the average O_2 molar concentration measured by GC to the *in-situ* optode O_2 molar concentration, and the last term corrects for over- or under-saturation in O_2 due to physical processes (here super-saturation of dissolved gases from the hydropower plant). We illustrate the corrections in the results and discussion section.

Gross primary production was related to photosynthetic active radiations (PAR) with a rectangular hyperbola (Michaelis-Menten type model):

$$GPP = \frac{GPPmax\ PAR}{k_{PAR} + PAR} \quad (9)$$

with *GPPmax* being the maximum GPP, *PAR* photosynthetic active radiations (mol quanta m^{-2} day^{-1}), and k_{PAR} the *PAR* at which half the *GPPmax* was realised. The rectangular hyperbola model is related to the hyperbolic tangent model (Jassby and Platt 1976):

$$GPP = GPPmax \tanh(\alpha\ PAR\ /\ GPPmax) \quad (10)$$

with the initial slope $\alpha = GPPmax/k_{PAR}$ (Hootsmans and Vermaat 1994). Both models generally perform equally well with biologically meaningful parameters, k_{PAR} the onset of light saturation and α low light use efficiency (Hootsmans and Vermaat 1994). Note both PAR and GPP units must be converted in the same unit (g C m^{-2} day^{-1}) to calculate light use efficiency: 1 mol photon m^{-2} day^{-1} = 6.13 g C m^{-2} day^{-1} for PAR and 1 g O_2 m^{-2} day^{-1} = 0.375 g C m^{-2} day^{-1} for GPP (O'Gorman et al. 2016). Average light use efficiency may also be reported from daily integrated GPP and PAR.

Should photosynthesis and aerobic respiration dominate river metabolism, then the diel molar concentrations of O_2 and CO_2 (or similarly ΔO_2 and ΔCO_2) should be inversely related with a ratio approaching 1:1 (Vachon et al. 2019). The respiratory quotient may deviate from 1 depending on the degree of oxidation of the respired substrate (Berggren et al. 2012). Photosynthesis quotient may also depart from 1 if the assimilation of nutrients (especially NO_3) is taken into account in the stoichiometric photosynthetic reaction (Stumm and Morgan 1981, p. 193-194; Demars and Edwards 2007). CO_2 may also enter the carbonate equilibrium (depending on pH) within 20-200 s (Zhang et al. 1995) and thus in base rich rivers the ΔO_2:ΔDIC ratio would be more relevant (Stumm and Morgan 1981).

3. Case study

The River Otra flows through forests in an alpine landscape in southern Norway and is extensively used for hydropower production with water reservoirs and water transfers (Rørslett 1988, Wright et al. 2017). The studied section drains about 1900 km^2, mostly through Brokke hydropower plant (Fig. 1), and discharge is heavily regulated with characteristic diel changes following electricity demand (Wright et al. 2017). The hydropower plant effluent can also release water highly supersaturated in dissolved gases posing risks to fish health (e.g. Lennox et al. 2022, Stenberg et al. 2022). Supersaturation is due to air entrainment in the secondary water intakes followed by dissolution in pressure tunnels. Supersaturation depends on the source of water (secondary stream intakes *versus* reservoirs) and hydraulic head and is mostly independent of discharge (Pulg et al. 2016a, Stenberg et al. 2022). In addition to the controlled flow, the studied river reach Rysstad – Straume shows profuse growth of the perennial aquatic plant *Juncus bulbosus* (L.) 3 to 7.8 km downstream of the hydropower plant effluent where it covered about 66% of the channel in June 2020 with a standing biomass of 57±8 g C m^{-2} (Fig. 1; Rørslett 1988).

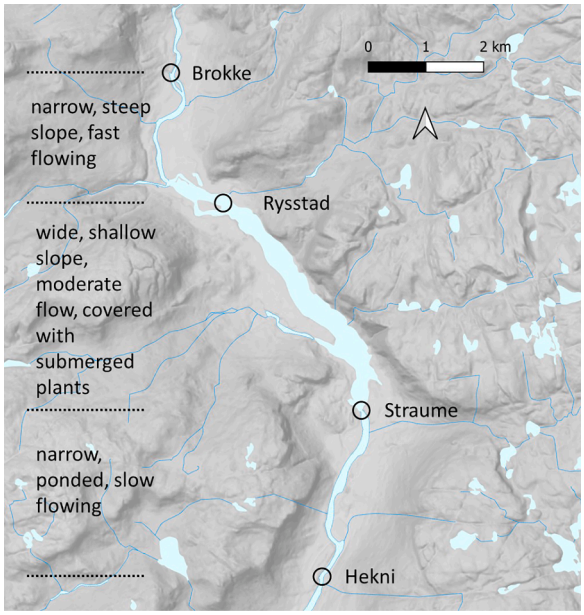

Fig. 1. Study area with three contrasting river sections. The hydropower plant effluent is at Brokke and the dissolved oxygen sensor was placed downstream at Straume. There is a dam at Hekni controlling the water level at least up to Straume.

Total dissolved gas (TDG) was recorded every 30 min in the effluent (deep open canal) of the hydropower plant with a Total Gas Analyzer 3.0 (Fisch- und. Wassertechnik; Pulg et al. 2016a, Pulg et al. 2016b), based on the Weiss-saturometer principle (Weiss, 1970). The Total Gas Analyzer measures TDG pressure in a submerged gas permeable silicon hose connected to an underwater pressure sensor and an atmospheric pressure sensor above the surface water. The saturation is measured as the percent dissolved air in the water relative to expectation from ambient air pressure. The saturometer has an accuracy of ± 10 hPa, which is approximately ± 1 % TDG.

A monitoring station placed at Straume (Fig. 1) logged at 15-minute intervals dissolved oxygen and water temperature (Xylem-Aanderaa optode 4831), photosynthetic active radiation above the water surface (LICOR, Quantum LI190R-L), air temperature and atmospheric pressure (Barometer RM Young 061302V) using a Campbell datalogger (CR1000X). The oxygen sensor was inserted in a white plastic pipe fixed to the bridge and protruding in the main current at about 1 m depth. The oxygen optode was calibrated in the lab and cross-calibrated in saturated river water using an air bubbler in a small tank by the side of the river, as in previous studies (e.g. Demars 2019).

We studied three diel cycles in August 2019 (4-5th) and June 2020 (12-13th and 25-26th) with varying levels of gas supersaturation. Water samples were collected at two sites every two hours over 24 hr on both sides of the river, 3 km (Rysstad) and 7.8 km (Straume) downstream the hydropower plant effluent where the river channel is more constrained (Fig. 1). Water bottles (120 mL) were filled to the rim and capped underwater with rubber seals, then crimped. Mercuric chloride ($HgCl_2$) was immediately added to stop biological processes (100µL of a half saturated solution per 120 mL bottle). We checked that the addition of $HgCl_2$ did not affect the determination of CO_2 (Borges et al. 2019, Koschorreck et al. 2021). The samples were kept cool (+4°C) and in the dark until the day of gas analysis at end of the field season. The samples were warmed and weighed at room temperature prior to sample

pre-processing. A headspace was created by gently backfilling 30-40 mL helium into the bottles through a short needle while removing the water through a 50 mL open syringe (without plunger) with a long needle. The helium supply was first removed, and when the water stopped rising in the syringe due to the helium overpressure (0.5 bar), the long needle was brought up in the headspace to degas excess helium bubbling in the syringe. This method assumes that there is no gas exchange between the water and the headspace prior to shaking the bottles. As soon as the bubbling stopped, the long needle was removed, the samples were weighed again (to determine the volume of water removed from the bottle) and shaken horizontally at 150 rpm for one hour. Water temperature and atmospheric pressure in the laboratory were recorded during the gas equilibration phase.

The bottles were then placed in an autosampler (GC-Pal, CTC, Switzerland) coupled to a gas chromatograph (Model 7890A, Agilent, Santa Clara, CA, US). Headspace gas was sampled (approx. 2 mL) by a hypodermic needle connected to a peristaltic pump (Gilson Minipuls 3), which connects the autosampler with two 250 µL heated sampling loops of the GC. The GC is equipped with 20-m wide-bore (0.53 mm) Poraplot Q column for separation of CH_4, CO_2 and N_2O and a 60 m wide-bore Molsieve 5Å PLOT column for separation of O_2, N_2 and Ar, both operated at 38°C and with He as carrier gas. CO_2, O_2, N_2 and Ar were measured with a thermal conductivity detector (TCD). Certified standards of CO_2, N_2O, and CH_4 in He were used for calibration (AGA, Germany). The GC analytical error was lower than 2%. Air was used for calibrating O_2, N_2 and Ar. Dissolved gas concentrations were calculated similarly to Yang et al. 2015 using the gas solubilities of Carroll et al. (1991) for CO_2, Weiss and Price (1980) for N_2O, Yamamoto et al. (1976) for CH_4, Millero et al. (2002) for O_2, and Hamme and Emerson (2004) for N_2 and Ar.

The determination of oxygen and total dissolved gases by gas chromatography (GC) and sensors should give the same results (Fickeisen et al. 1975), but our GC-headspace results were systematically higher (+4%) than those recorded by the calibrated sensors in a preliminary study (Demars et al. 2021). The O_2:Ar ratio should not be affected much by these discrepancies, however, and our back-calculation of the argon concentration using the O_2 optode circumvented this systematic bias (see above). The combined sampling and analytical error of our GC-headspace method, as given by coefficients of variation (standard deviation / average), was about 0.3% for O_2, N_2, Ar and the O_2:Ar ratio, 2% for N_2O, 5% for CH_4 and 5% (without an outlier) for CO_2, based on five samples collected at the same place and time in the River Otra. The two grab samples, collected on each side of the river for the GC-headspace method, were averaged prior to calculating stream metabolism.

Mean water depth z (range 1.3-1.8 m) between Rysstad and Straume was deduced from a bathymetric survey (metered sticks and sonar data crisscrossing the river channel), water level sensors (Onset HOBO data loggers U20L-04) and discharge at Straume (Pathak and Demars 2023). Discharge was derived from a flow routing model calibrated with two gauging stations situated about 7.5 km upstream (Brokke) and 3 km downstream (Hekni dam) of Straume study site – Fig. 1; Pathak and Demars 2023. Solute velocity was determined from peaks in total dissolved gases and related to discharge (Pathak and Demars 2023). Solute velocity ranged 0.1-0.5 m s^{-1} in the studied reach.

The gas exchange coefficient k=0.36 day^{-1} was estimated between Rysstad and Straume using floating flux chambers (Bastviken et al. 2015) and was found to be independent of water temperature and discharge (Pathak and Demars 2023). Here, we also calculated the gas exchange rate using the argon concentrations of our three diel studies for the same parcel of water (i.e. taking into account solute time lag) between Rysstad and Straume (our studied reach). We found similar results to the floating flux chambers: 0.11±0.04, 0.14±0.11 and 0.46±0.19 per day for the 4th August 2019, 12th and 25th June 2020, respectively. The application of a classical one-station model was not appropriate at the study site due to slow gas exchange (gas exchange coefficient <1 day^{-1}), rapid changes in flow combined with long solute travel time (Pathak and Demars 2023). The standardisation of the oxygen concentrations with argon should, however, remove most of the changes in dissolved oxygen due to the hydropower plant, both in terms of physical gas supersaturation and changes in travel time with oxygen and argon moving at the same pace. Thus we expected to find similar results to our two-station model when applicable (Pathak and Demars 2023), despite the oxygen sensor footprint at Straume being far longer than the studied reach. Note the first section Brokke – Rysstad was narrower (wetted width 107 m), steeper (slope 0.0016 m/m) and shallower (depth 0.64 m) with faster solute velocity (0.73 m s^{-1}) and gas transfer velocity (K_L=5 m day^{-1} derived from Pulg et al. 2018) than the reach Rysstad-Straume with wetted width 316 m, slope partly controlled by Hekni dam, depth 1.33 m, solute velocity 0.14 m s^{-1} and gas transfer velocity 0.48 m day^{-1} (calculations for Q=50 m^3 s^{-1}) – more details in Pathak and Demars (2023).

The stream metabolism calculations were done in Microsoft Excel assuming measurement errors of three key parameters were normally distributed with standard deviations of 0.1 mg O_2 L^{-1} for the corrected oxygen concentrations, 0.15 m for depth and 0.07 day^{-1} for the gas exchange rate. Uncertainties were propagated using 1000 Monte Carlo simulations. The median of the 1000 runs provided a numerical solution for ER and GPP. The 2.5th and 97.5th centiles provided a 95% confidence interval. Random draws were carried out with the inverse of the normal cumulative distribution for a specified mean and standard deviation using the function NORM.INV(RAND(),mean, standard deviation) and the calculations repeated automatically with Data Table. Excel spreadsheets are provided in Supporting Information. The parameters of the light models were fitted with a non-linear regression model in R 4.0.0 using the nls function (R Core Team 2020). Model summary reported the parameter values and their standard errors.

The river Otra has low alkalinity 54±7 µmol L^{-1}, low specific electric conductivity (about 10 µS cm^{-1}) and low total organic carbon (generally TOC <2 mg C L^{-1}) – Moe and Demars (2017). We used seacarb to calculate HCO_3 and DIC from alkalinity (average) and CO_2 (GC data) with Millero (2010) constants (salinity range 1-50 PSU, temperature range 0-50°C) – (Gattuso et al., 2021, Orr et al. 2015). The pH values (range 6.4-6.9) also reported by seacarb for our samples were very similar (within 0.1 pH unit) to the method of Koschorreck et al 2021 using equilibrium constants for freshwater. HCO_3 remained constant during the CO_2 diel cycle (54 and 43 µmol L^{-1} in 2019 and 2020, respectively), i.e. there was no evidence of CO_2 entering the carbonate equilibrium, and thus the slope of the O_2:CO_2 and O_2:DIC ratios were the same.

4. Results and discussion

4.1. Method development

Dissolved oxygen concentrations determined by gas chromatography overestimated *in-situ* optode measured O_2 concentration on average by 4% in August 2019 and underestimated concentrations on average by 7% in June 2020 (Fig. 2). The applied corrections, using the O_2:Ar ratio of the grab samples and *in-situ* Ar concentrations derived from optode O_2 measurements aligned the GC oxygen concentrations with the *in-situ* measured O_2 concentrations (Fig. 2). In August 2019, the amplitude and corrected absolute concentration of O_2 remained similar as there was little evidence of physical supersaturation from the effluent of the hydropower plant (105-110% total dissolved gas saturation, Demars et al. 2021) and E*p*Ar≈1.01 at Straume. In June 2020, the diel amplitude and absolute values of the corrected oxygen concentrations were much smaller than the one measured by the optode because of very high physical supersaturation of total dissolved gases in the effluent of the hydropower plant: 170% on the 12-13th June and 145% on the 25-26th June leading to E*p*Ar≈1.13 at Straume. During such high supersaturation events the water fizzes downstream of the effluent leading to

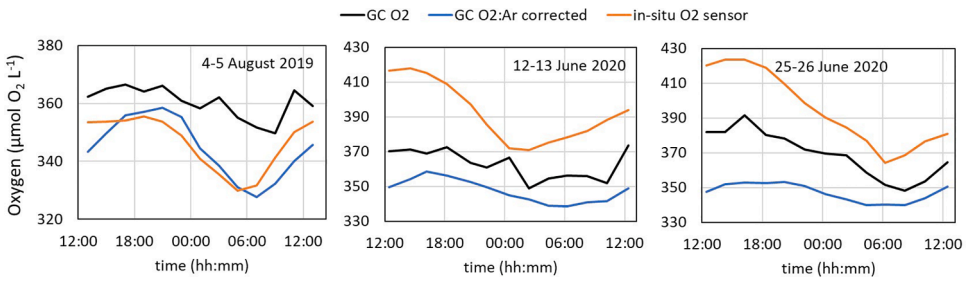

Fig. 2. Oxygen concentrations determined by gas chromatography (GC) with and without O_2:Ar correction at Straume, and comparison with *in-situ* oxygen sensor.

substantial losses in total dissolved gas supersaturation within the first three kilometres (Pulg et al. 2018).

Mean (±sd) concentrations of CO_2 three kilometres downstream the effluent at Rysstad (54±20, 27±3, 30±4 µmol CO_2 L^{-1}) were similar to those at Straume (44±9, 30±7, 33±7 µmol CO_2 L^{-1}) on the three sampling dates, independently of total dissolved gas saturation. This is not so surprising as at this site, CO_2 concentrations are strongly driven by ecosystem metabolism (net ecosystem production). The standardisation of the oxygen curves through the O_2:Ar ratio provided sinusoidal curves as expected from the low gas exchange rate (<1 day^{-1}) and high biological activity (Fig. 2, Demars et al. 2015), allowing for estimates of NEP.

NEP responded to light (Fig. 3), becoming negative at night when respiration exceeded photosynthesis. Assuming respiration observed at night was constant throughout the day, we demonstrate that GPP was highly related to light availability (photosynthetic active radiation, Fig. 4). We also found a strong relationship between O_2 and CO_2 concentrations with a negative slope approaching -1 (Fig. 5), as expected

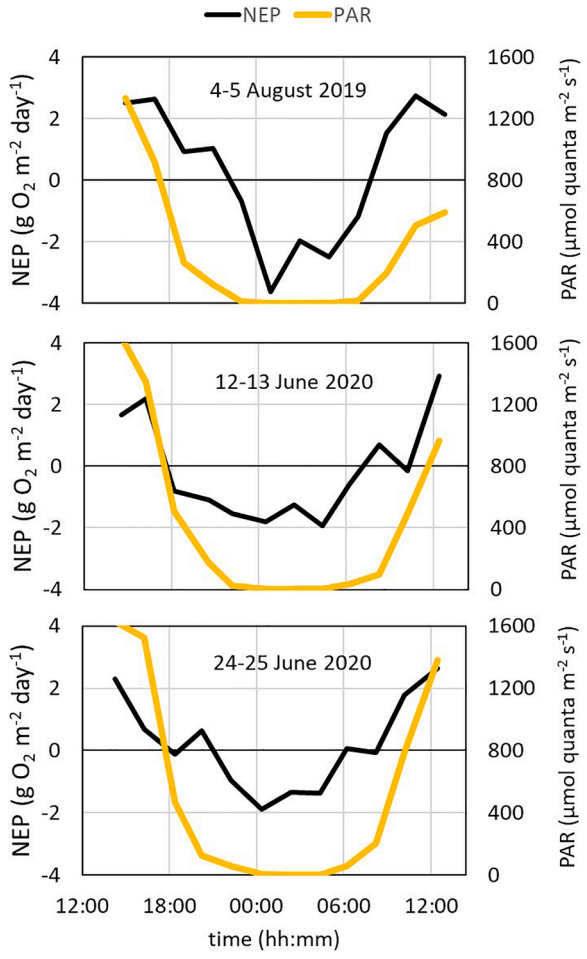

Fig. 3. Diel changes in net ecosystem production (NEP) and photosynthetic active radiation (PAR)

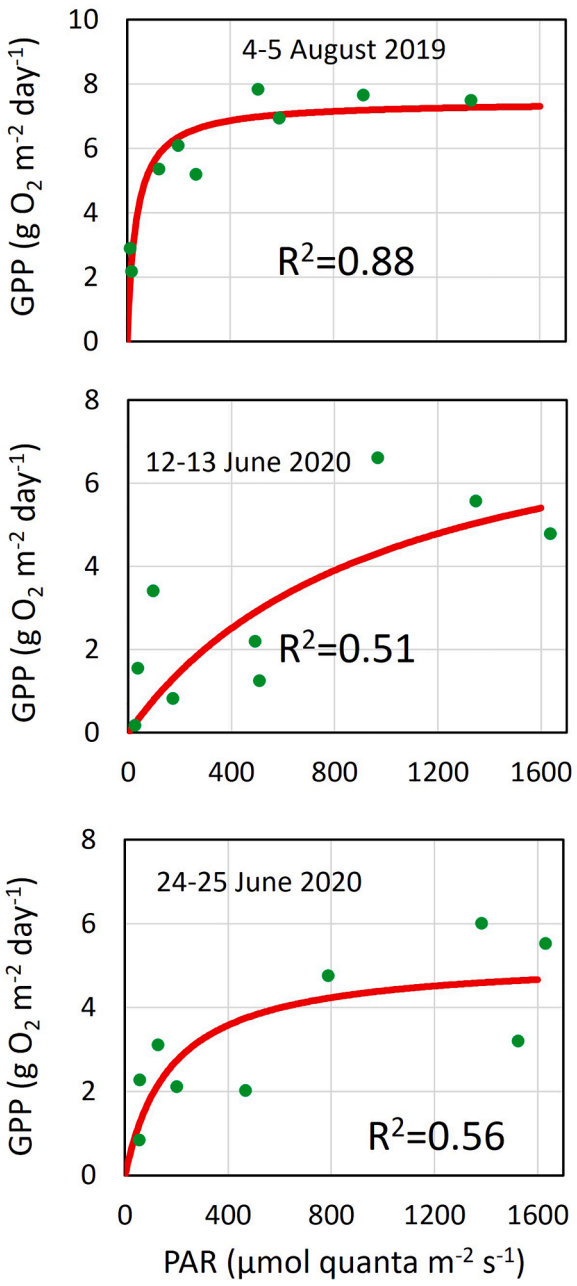

Fig. 4. Gross primary production as a function of light (photosynthetic active radiations), dots are observed data and curves are derived from a fitted Michaelis-Menten type model.

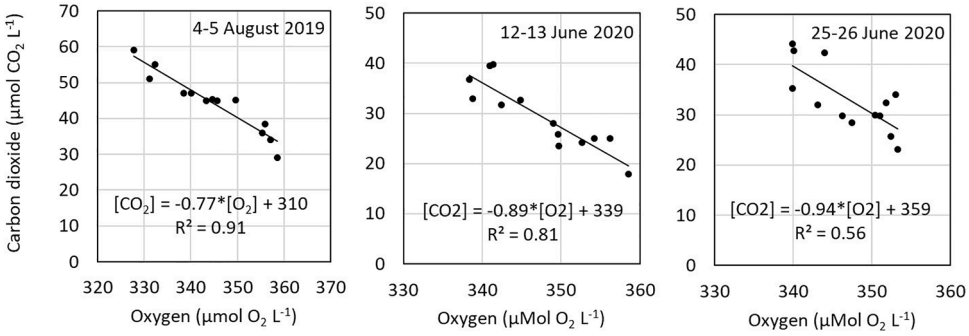

Fig. 5. Tight inverse relationships close to the expected 1:1 ratio between carbon dioxide and oxygen molar concentrations after O_2:Ar correction. Note, HCO_3 concentrations remained constant and carbonate concentrations were negligible during the CO_2 diel cycle in the River Otra. Thus the slope of the O_2:CO_2 and O_2:DIC ratios were the same.

Table 1
River Otra conditions (range) and metabolic estimates from Monte Carlo simulations (median and 95% confidence interval). * just outside the hydropower plant effluent at Brokke

Dates	TDG* %	Discharge $m^3\ s^{-1}$	Velocity $m\ s^{-1}$	Depth m	ER $g\ O_2\ m^2\ day^{-1}$	GPP $g\ O_2\ m^2\ day^{-1}$
4-5 August 2019	105-110	28-72	0.09-0.19	1.29-1.38	-3.9 (-3.1 to -4.8)	5.8 (4.6-7.0)
12-13 June 2020	160-180	129-201	0.30-0.49	1.50-1.75	-2.4 (-1.9 to -2.8)	2.9 (2.4-3.4)
25-26 June 2020	140-150	159-228	0.39-0.53	1.60-1.81	-2.1 (-1.8 to -2.6)	3.3 (2.7-4.0)

Table 2
Daily light (PAR, photosynthetic active radiations), daily light use efficiency (E=GPP/PAR), maximum gross primary production (GPPmax), the onset of light saturation (k_{PAR}) and low light use efficiency (α=GPPmax/k_{PAR}). Uncertainties are 95% CI for E and standard errors for GPPmax and k_{PAR}.

Dates	PAR mol quanta $m^{-2}\ day^{-1}$	E %	GPPmax $g\ O_2\ m^{-2}\ day^{-1}$	k_{PAR} µmol quanta $m^{-2}\ s^{-1}$	α %
4-5 August 2019	28.5	1.3 ±0.3	7.4 ±0.4	35 ±13	15 ±5.6
12-13 June 2020	34.5	0.5 ±0.09	9.1 ±5.9	987 ±1290	0.7 ±1.0
25-26 June 2020	43.6	0.4 ±0.06	5.3 ±1.0	188 ±137	6.9 ±5.2

when photosynthesis and aerobic respiration dominate river metabolism and CO_2 is not assimilated by the carbonate equilibrium (Vachon et al. 2019; see *Theory* section above). The slopes were slightly lower than expected possibly due to higher respiration activity during daylight hours (Hotchkiss and Hall 2014) or a combination of other factors (see Theory section). The slopes were relatively independent of the degree of total dissolved gas supersaturation in the effluent, suggesting the hydropower plant did not affect much CO_2 supersaturation at the study site (Straume). This is likely due to the higher evasion rate of CO_2 than O_2 when the water is fizzing (Hall and Madinger 2018) between Brokke and Rysstad.

The estimated metabolic rates (Table 1) were slightly larger in August 2019 than in June 2020, mostly due to higher temperature (Demars et al. 2023) rather than changes in depth and light penetration (Binzer et al. 2006, Demars et al. 2023, Hall et al. 2015). The GPPmax (median ± 95% CI) derived from a Michaelis-Menten model was 7.4 ±0.4 g O_2 m^2 day^{-1} (Fig. 4) which is similar to 9.2±0.3 g O_2 m^2 day^{-1} derived from the two-station method on 5-7th August 2019 (Pathak and Demars 2023). The onset of light saturation, k_{PAR} = 35±13 µmol quanta m^{-2} s^{-1}, was significantly lower than the two-station method (133±13 µmol quanta m^{-2} s^{-1}). ER and GPP (median ± 95% CI) were also statistically similar with the two-station method (5th August 2019) reporting -3.7±0.2 and 4.2±0.2 g O_2 m^2 day^{-1}, respectively (Pathak and Demars 2023). Overall, our estimates of summer daily photosynthesis exceeded respiration which was expected at this time of year (short night, high light) in a sandy riverbed (little CO_2 production from organic matter decomposition) with a relatively high standing biomass of submerged *J. bulbosus* throughout the water column (average biomass 50 g C m^{-2}). Photosynthesic rates were relatively high (60-78th centile) and community respiration low (20-33th centile) relative to a global compilation of 222 streams during summer time or dry season (Demars et al. 2016). The metabolic rates were however relatively low to modest for rivers dominated by submerged vascular plants (e.g. Edwards and Owens 1962, Kelly et al. 1983, Odum 1957). The sampling frequency (every two hours) was too low to return accurate light parameters. This led to disparate results for low light use efficiencies (Table 2) and a large difference with the two-station method in 2019 (α=4.9±0.5%). The daily light use efficiencies were more comparable (Table 2), also with the two-station method in 2019 (E=0.9±0.04%), and similar to other rivers for which a comparable method was used (Kirk et al. 2021).

The simplicity of the current approach stands in sharp contrast to the complexity of the study site and the two-station method only applicable during days without significant supersaturation from the hydropower plant (Pathak and Demars 2023, Payn et al. 2017). While argon has been used for gas exchange studies in streams (e.g. Hall and Madinger 2018, Knapp et al. 2019, Ulseth et al. 2019), it has not been used for stream metabolism and thus prevented the estimation of ecosystem respiration (e.g. Hall et al. 2015). The argon accounting method can provide an independent check on alternative correction and modelling approach for long term time series (e.g. Roley et al. 2023).

Our GC approach requires the use of an oxygen optode to anchor Ar and O_2 concentrations measured by the headspace-GC method to well-calibrated *in-situ* O_2 measurements. *In-situ* measurements by membrane inlet mass spectrometry (MIMS) have proven extremely accurate to determine a wide range of dissolved gas concentrations and O_2:Ar ratio (e.g. Cassar et al. 2009, Kaiser et al. 2005) and circumvent

problems with grab sampling and the headspace GC method. Portable MIMS are now more available and open new opportunities for *in-situ* studies (e.g. Popp et al. 2021).

4.2. Aquatic plant ecology

Carbon dioxide concentrations in the water column were halved at the peak of photosynthesis (Fig. 5) and CO_2 concentrations (20-60 μmol CO_2 L^{-1}) were well below the level necessary to saturate underwater photosynthesis of the leaf apparatus of *J. bulbosus* (over 500 μmol CO_2 L^{-1}, Roelofs et al. 1984, Sand-Jensen 1987). Svedang (1992) reported an increase in *J. bulbosus* growth rate when CO_2 was added (×10) to the water column in a lake with highly organic sediment (potentially high sediment CO_2 production) and background CO_2 concentration around 50 μmol CO_2 L^{-1}. This may partly be due to the fact that *J. bulbosus* can alleviate CO_2 limitation by efficient internal gas recycling and CO_2 root uptake (Wetzel et al. 1984, Wetzel et al. 1985) with sediment pore water concentrations averaging 170 μmol CO_2 L^{-1} (Moe and Demars 2017) and suggests that other nutrients may be co-limiting for *J. bulbosus* growth (Moe et al. 2021).

Since *J. bulbosus* is a perennial plant, the final yield is more constrained by the dampening of spring freshet following water regulation (Gurnell 2014, Rørslett 1988, Rørslett et al. 1989). Over an annual cycle, light availability and temperature were also found to constrain photosynthesis, and plant cover (or standing biomass) could recover from mechanical plant harvesting within two-three years (Demars et al. 2023).

5. Conclusion

We devised a new, parsimonious approach based on O_2:Ar ratios to estimate river metabolism. The method corrects for imprecision of headspace measurements in grab samples and for under- or supersaturation of total dissolved gases due to physical processes, such as bubble mediated degassing, lateral inflow, or cooling or warming in rivers with low gas exchange rates downstream of thermal effluents. The results compared well with a more sophisticated two-station model based on O_2 mass balance alone, which could not be applied during dissolved gas supersaturation events (Demars et al. 2023). Ecosystem respiration and gross primary production of *J. bulbosus* were determined under varying supersaturation events. The use of the O_2:Ar approach may become more applicable with the emergence of portable mass inlet mass spectrometers (MIMS).

Declaration of Competing Interest

The authors declare that they have no known competing financial interests or personal relationships that could have appeared to influence the work reported in this paper.

Data availability

We have made our data to calculate metabolism available in Supplementary Information

Acknowledgements

We thank Gjermund Espetveit (Otra Kraft) for providing flow data and Torstein Try for providing the boats; Ulrich Pulg and Sebastian Stranzl for providing TDG data; Odd Arne Skogan for setting up the Campbell logging station; Knut Olav Oppstad for providing sonar bathymetric data; Kirstine Thiemer, Susanne Schneider, François Clayer, Emmanuel Bergan, Astrid Torske, Eirin Aasland for help collecting water samples, bathymetric and plant data, as well as CO_2 flux with the floating chambers; Gaute Velle, Robert Hall Jr. and an anonymous referee for constructive comments on the manuscript. BOLD gratefully acknowledge the Research Council of Norway (297202/E10), the German Federal Ministry of Education and Research (033WU005), the French Agence National de Recherche (N°ANR-18-IC4W-0004-06), the South African Water Research Commission (K5/2951) and Fundação Araucária in Brazil (N° 186/2019) for funding of MadMacs (Mass development of aquatic macrophytes - causes and consequences of macrophyte removal for ecosystem structure, function, and services) in the frame of the collaborative inter-national consortium of the 2017 call of the Water Challenges for a Changing World Joint Programme Initiative (Water JPI). Additional funding was provided by Krypsiv på Sørlandet and the Norwegian institute for water research (NIVA).

Supplementary materials

Supplementary material associated with this article can be found, in the online version, at doi:10.1016/j.watres.2023.120842.

References

Appling, A.P., Hall Jr., R.O., Yackulic, C.B., Arroita, M, 2018a. Overcoming equifinality: leveraging long time series for stream metabolism estimation. J. Geophys. Res. 123, 624–645.

Appling, A.P., Read, J.S., Winslow, L.A., Arroita, M., Bernhardt, E.S., Griffiths, N.A., Hall Jr, R.O., Harvey, J.W., Heffernan, J.B., Stanley, E.H, 2018b. The metabolic regimes of 356 rivers in the United States. Sci. Data 5, 180292.

Asher, W.E., Wanninkhof, R., 1998. The effect of bubble-mediated gas transfer on purposeful dual-gaseous tracer experiments. J. Geophys. Res. Oceans 103 (C5), 10555–10560.

Bastviken, D., Sundgren, I., Natchimuthu, S., Reyier, H., Galfalk, M., 2015. Technical Note: Cost-efficient approaches to measure carbon dioxide (CO_2) fluxes and concentrations in terrestrial and aquatic environments using mini loggers. Biogeosciences 12 (12), 3849–3859.

Battin, T.J., Lauerwald, R., Bernhardt, E.S., Bertuzzo, E., Gener, L.G., Hall Jr,, R.O., Hotchkiss, E.R., Maavara, T., Pavelsky, T.M., Ran, L, 2023. River ecosystem metabolism and carbon biogeochemistry in a changing world. Nature 613 (7944), 449–459.

Berggren, M., Lapierre, J.F., del Giorgio, P.A., 2012. Magnitude and regulation of bacterioplankton respiratory quotient across freshwater environmental gradients. Isme J. 6 (5), 984–993.

Bernhardt, E.S., Savoy, P., Vlah, M.J., Appling, A.P., Koenig, L.E., Hall, R.O., Arroita, M., Blaszczak, J.R., Carter, A.M., Cohen, M., Harvey, J.W., Heffernan, J.B., Helton, A.M., Hosen, J.D., Kirk, L., McDowell, W.H., Stanley, E.H., Yackulic, C.B., Grimm, N.B., 2022. Light and flow regimes regulate the metabolism of rivers. Proc. Nat. Acad. Sci. USA 119 (8), e2121976119.

Binzer, T., Sand-Jensen, K., Middelboe, A.-L., 2006. Community photosynthesis of aquatic macrophytes. Limnol. Oceanogr. 51 (6), 2722–2733.

Borges, A.V., Darchambeau, F., Lambert, T., Morana, C., Allen, G.H., Tambwe, E., Sembaito, A.T., Mambo, T., Wabakhangazi, J.N., Descy, J.P., Teodoru, C.R., Bouillon, S., 2019. Variations in dissolved greenhouse gases (CO_2, CH_4, N_2O) in the Congo River network overwhelmingly driven by fluvial-wetland connectivity. Biogeosciences 16 (19), 3801–3834.

Carroll, J.J., Slupsky, J.D., Mather, A.E., 1991. The solubility of carbon dioxide in water at low pressure. J. Phys. Chem. Ref. Data 20 (6), 1201–1209.

Cassar, N., Barnett, B.A., Bender, M.L., Kaiser, J., Hamme, R.C., Tilbrook, B., 2009. Continuous high-frequency dissolved O_2/Ar measurements by equilibrator inlet mass spectrometry. Anal. Chem. 81 (5), 1855–1864.

Craig, H., Hayward, T., 1987. Oxygen supersaturation in the ocean: biological versus physical contributions. Science 235 (4785), 199–202.

Craig, H., Wharton, R.A., McKay, C.P., 1992. Oxygen supersaturation in ice-covered Antarctic lakes: biological versus physical contributions. Science 255 (5042), 318–321.

Cross, W.F., Baxter, C.V., Rosi-Marshall, E.J., Hall, R.O., Kennedy, T.A., Donner, K.C., Kelly, H.A.W., Seegert, S.E.Z., Behn, K.E., Yard, M.D., 2013. Food-web dynamics in a large river discontinuum. Ecological Monographs 83 (3), 311–337.

Dawson, J.J.C., 2013. Ecosystem Services and Carbon Sequestration in the Biosphere, eds. Springer Science, Dordrecht, pp. 183–208.

Demars, B.O.L., 2019. Hydrological pulses and burning of dissolved organic carbon by stream respiration. Limnol. Oceanogr. 64, 406–421.

Demars, B.O.L., Dörsch, P., Thiemer, K., Clayer, F., Schneider, S.C., Stranzl, S.F., Pulg, U., Velle, G., 2021. Hydropower: gas supersaturation and the role of aquatic plant photosynthesis for fish health. Rapport 7633-2021. Norwegian Institute for Water Research, Oslo.

Demars, B.O.L., Edwards, A.C., 2007. Tissue nutrient concentrations in freshwater aquatic macrophytes: high inter-taxon differences and low phenotypic response to nutrient supply. Freshwater Biol. 52 (11), 2073–2086.

Demars, B.O.L., Friberg, N., Thornton, B., 2020. Pulse of dissolved organic matter alters reciprocal carbon subsidies between autotrophs and bacteria in stream food webs. Ecological Monographs 90 (1), e01399.

Demars, B.O.L., Gislason, G.M., Olafsson, J.S., Manson, J.R., Friberg, N., Hood, J.M., Thompson, J.J.D., Freitag, T.E., 2016. Impact of warming on CO_2 emissions from streams countered by aquatic photosynthesis. Nat. Geosci. 9 (10), 758–761.
Demars, B.O.L., Manson, J.R., 2013. Temperature dependence of stream aeration coefficients and the effect of water turbulence: a critical review. Water Res. 47 (1), 1–15.
Demars, B.O.L., Schneider, S.C., Thiemer, K., Dörsch, P., Pulg, U., Stranzl, S.F., Velle, G., Pathak, D.. Light and temperature controls of aquatic plant photosynthesis downstream of a hydropower plant and the effect of plant removal. https://doi.org/10.2139/ssrn.4524655.
Demars, B.O.L., Thompson, J., Manson, J.R., 2015. Stream metabolism and the open diel oxygen method: Principles, practice, and perspectives. Limnol. Oceanogr. Methods 13 (7), 356–374.
Edwards, R.W., Owens, M., 1962. The effect of plants on river conditions. IV. The oxygen balance of a chalk stream. J. Ecol. 50, 207–220.
Emerson, S., Quay, P., Stump, C., Wilbur, D., Knox, M., 1991. O_2, Ar, N_2 and 222Rn in surface waters of the subarctic ocean: Net biological O_2 production. Global Biogeochem. Cycles 5 (1), 49–69.
Eveleth, R., Timmermans, M.L., Cassar, N., 2014. Physical and biological controls on oxygen saturation variability in the upper Arctic Ocean. J. Geophys. Res. Oceans 119 (11), 7420–7432.
Fickeisen, D.H., Schneider, M.J., Montgomery, J.C., 1975. A comparative evaluation of the Weiss saturometer. Trans. Am. Fisheries Soc. 104 (4), 816–820.
Gattuso, J.-P., Epitalon, J.-M., Lavigne, H., Orr, J.C.. seacarb: seawater carbonate chemistry, version 3.3.0. https://www.rdocumentation.org/packages/seacarb/versions/3.3.2.
Grace, M.R., Giling, D.P., Hladyz, S., Caron, V., Thompson, R.M., Mac Nally, R., 2015. Fast processing of diel oxygen curves: Estimating stream metabolism with BASE (BAyesian Single-station Estimation). Limnol. Oceanogr. Methods 13, 103–114.
Grill, G., Lehner, B., Thieme, M., Geenen, B., Tickner, D., Antonelli, F., Babu, S., Borrelli, P., Cheng, L., Crochetiere, H., Macedo, H.E., Filgueiras, R., Goichot, M., Higgins, J., Hogan, Z., Lip, B., McClain, M.E., Meng, J., Mulligan, M., Nilsson, C., Olden, J.D., Opperman, J.J., Petry, P., Liermann, C.R., Saenz, L., Salinas-Rodriguez, S., Schelle, P., Schmitt, R.J.P., Snider, J., Tan, F., Tockner, K., Valdujo, P. H., van Soesbergen, A., Zarfl, C., 2019. Mapping the world's free-flowing rivers. Nature 569 (7755), 215–221.
Gurnell, A., 2014. Plants as river system engineers. Earth Surf. Processes Landforms 39 (1), 4–25.
Hall Jr, R.O., Kennedy, T.A., Rosi-Marshall, E.J, 2012. Air–water oxygen exchange in a large whitewater river. Limnol. Oceanogr. 2, 1–11.
Hall Jr., R.O., Tank, J.L., Baker, M.A., Rosi-Marshall, E.J., Hotchkiss, E.R, 2016. Metabolism, gas exchange, and carbon spiraling in rivers. Ecosystems 19 (1), 73–86.
Hall Jr., R.O., Yackulic, C.B., Kennedy, T.A., Yard, M.D., Rosi-Marshall, E.J., Voichick, N., Behn, K.E, 2015. Turbidity, light, temperature, and hydropeaking control primary productivity in the Colorado River, Grand Canyon. Limnol. Oceanogr. 60 (2), 512–526.
Hall, R.O., Madinger, H.L., 2018. Use of argon to measure gas exchange in turbulent mountain streams. Biogeosciences 15, 3085–3092.
Hamme, R.C., Emerson, S.R., 2004. The solubility of neon, nitrogen and argon in distilled water and seawater. Deep-Sea Research Part I-Oceanogr. Res. Papers 51 (11), 1517–1528.
Holtgrieve, G.W., Schindler, D.E., Branch, T.A., A'Mar, Z.T, 2010. Simultaneous quantification of aquatic ecosystem metabolism and reaeration using a Bayesian statistical model of oxygen dynamics. Limnol. Oceanogr. 55 (3), 1047–1063.
Holtgrieve, G.W., Schindler, D.E., Jankowski, K., 2016. Comment on Demars et al. 2015, "Stream metabolism and the open diel oxygen method: Principles, practice, and perspectives. Limnol. Oceanogr. Methods 14 (2), 110–113.
Hootsmans, M.J.M., Vermaat, J.E., 1994. In: Vierssen, W., Hootsmans, M., Vermaat, J. (Eds.), Lake Veluwe, a Macrophyte-Dominated System Under Eutrophication Stress, eds. Kluwer, Netherlands, pp. 62–117.
Hotchkiss, E.R., Hall Jr., R.O., 2014. High rates of daytime respiration in three streams: Use of delta O-18(O2) and O-2 to model diel ecosystem metabolism. Limnol. Oceanogr. 59 (3), 798–810.
Hotchkiss, E.R., Hall Jr., R.O., Sponseller, R.A., Butman, D., Klaminder, J., Laudon, H., Rosvall, M., Karlsson, J, 2015. Sources of and processes controlling CO_2 emissions change with the size of streams and rivers. Nat. Geosci. 8 (9), 696–699.
Howard, E., Emerson, S., Bushinsky, S., Stump, C., 2010. The role of net community production in air-sea carbon fluxes at the North Pacific subarctic-subtropical boundary region. Limnol. Oceanogr. 55 (6), 2585–2596.
Hussner, A., Stiers, I., Verhofstad, M., Bakker, E.S., Grutters, B.M.C., Haury, J., van Valkenburg, J., Brundu, G., Newman, J., Clayton, J.S., Anderson, L.W.J., Hofstra, D, 2017. Management and control methods of invasive alien freshwater aquatic plants: a review. Aquatic Botany 136, 112–137.
Jassby, A.D., Platt, T., 1976. Mathematical formulation of the relationship between photosynthesis and light for phytoplankton. Limnol. Oceanogr. 21 (4), 540–547.
Kaiser, J., Reuer, M.K., Barnett, B., Bender, M.L., 2005. Marine productivity estimates from continuous O_2/Ar ratio measurements by membrane inlet mass spectrometry. Geophys. Res. Lett. 32 (19), L19605.
Kelly, M.G., Thyssen, N., Moeslund, B., 1983. Light and the annual variation of oxygen- and carbon-based measurements of productivity in a macrophyte-dominated river. Limnol. Oceanogr. 28 (3), 503–515.
Kirk, L., Hensley, R.T., Savoy, P., Heffernan, J.B., Cohen, M.J., 2021. Estimating benthic light regimes improves predictions of primary production and constrains light-use efficiency in streams and rivers. Ecosystems 24 (4), 825–839.
Knapp, J.L.A., Osenbruck, K., Brennwald, M.S., Cirpka, O.A., 2019. In-situ mass spectrometry improves the estimation of stream reaeration from gas-tracer tests. Sci. Total Environ. 655, 1062–1070.
Koschorreck, M., Prairie, Y.T., Kim, J., Marce, R., 2021. Technical note: CO2 is not like CH4 - limits of and corrections to the headspace method to analyse pCO(2) in fresh water. Biogeosciences 18 (5), 1619–1627.
Lennox, R.J., Thiemer, K., Vollset, K.W., Pulg, U., Stranzl, S., Nilsen, C.I., Haugen, T.O., Velle, G., 2022. Behavioural response of brown trout (Salmo trutta) to total dissolved gas supersaturation in a regulated river. Ecohydrology 15 (1), e2363.
Machler, L., Brennwald, M.S., Kipfer, R., 2013. Argon concentration time-series as a tool to study gas dynamics in the hyporheic zone. Environ. Sci. Technol. 47 (13), 7060–7066.
Manning, C.C., Stanley, R.H.R., Nicholson, D.P., Loose, B., Lovely, A., Schlosser, P., Hatcher, B.G., 2019. Changes in gross oxygen production, net oxygen production, and air-water gas exchange during seasonal ice melt in Whycocomagh Bay, a Canadian estuary in the Bras d'Or Lake system. Biogeosciences 16 (17), 3351–3376.
Marcarelli, A.M., Baxter, C.V., Mineau, M.M., Hall Jr., R.O., 2011. Quantity and quality: unifying food web and ecosystem perspectives on the role of resource subsidies in freshwaters. Ecology 92 (6), 1215–1225.
McCutchan, J.H., Saunders, I.J.F., Lewis, W.M., Hayden, M.G., 2002. Effects of groundwater flux on open-channel estimates of stream metabolism. Limnol. Oceanogr. 47 (1), 321–324.
Millero, F.J., 2010. Carbonate constant for estuarine waters. Mar. Freshwater Res. 61, 139–142.
Millero, F.J., Huang, F., Laferiere, A.L., 2002. Solubility of oxygen in the major sea salts as a function of concentration and temperature. Mar. Chem. 78 (4), 217–230.
Moe, T.F., Demars, B.O.L., 2017. Årsrapport krypsivovervåking 2017. Rapport 7202-2017. NIVA, Oslo.
Moe, T.F., Hessen, D.O., Demars, B.O.L., 2021. Juncus bulbosus tissue nutrient concentrations and stoichiometry in oligotrophic ecosystems: variability with seasons, growth forms, organs and habitats. Plants 10 (3), 441.
Nilsson, C., Reidy, C.A., Dynesius, M., Revenga, C., 2005. Fragmentation and flow regulation of the world's large river systems. Science 308 (5720), 405–408.
O'Gorman, E.J., Olafsson, O.P., Demars, B.O.L., Friberg, N., Gudbergsson, G., Hannesdottir, E.R., Jackson, M.C., Johansson, L.S., McLaughlin, O.B., Olafsson, J.S., Woodward, G., Gislason, G.M., 2016. Temperature effects on fish production across a natural thermal gradient. Global Change Biol. 22 (9), 3206–3220.
Odum, H.T., 1956. Primary production in flowing waters. Limnol. Oceanogr. 1 (2), 102–117.
Odum, H.T., 1957. Primary production measurements in eleven Florida springs and a marine turtle-grass community. Limnol. Oceanogr. 2, 85–97.
Orr, J.C., Epitalon, J.M., Gattuso, J.P., 2015. Comparison of ten packages that compute ocean carbonate chemistry. Biogeosciences 12 (5), 1483–1510.
Pathak, D., Demars, B.O.L., 2023. Metabolism modelling in rivers with unsteady flow conditions and transient storage zones. J. Geophys. Res. 128 e2022JG007245.
Payn, R.A., Hall, R.O., Kennedy, T.A., Poole, G.C., Marshall, L.A., 2017. A coupled metabolic-hydraulic model and calibration scheme for estimating whole-river metabolism during dynamic flow conditions. Limnol. Oceanogr. Methods 15 (10), 847–866.
Popp, A.L., Manning, C.C.M., Knapp, J.L.A., 2021. Rapid advances in mobile mass spectrometry enhance tracer hydrology and water management. Water Resour. Res. 57 (6) e2021WR029890.
Pulg, U., Espedal, E.O., Enqvist, M., Stranzl, S., 2022. Gassmetning i Otra nedenfor Brokke 2020 - 2021. Rapport 319. Uni Research Bergen, Uni Research Miljø LFI.
Pulg, U., Stranzl, S., Vollset, K.W., Barlaup, B.T., Olsen, E., Skår, B., Velle, G., 2016a. Gassmetning i Otra nedenfor Brokke kraftverk. Laboratorium for ferskvannsøkologi og innlandsfiske (LFI), UNI Research Miljø, Bergen.
Pulg, U., Vollset, K., Stranzl, S., Espedal, E.O., 2018. Gassmetning i Otra nedenfor Brokke 2016–2017 og muligheter for avbøtende tiltak. Uni Research Bergen, Uni Research Miljø LFI.
Pulg, U., Vollset, K.W., Velle, G., Stranzl, S., 2016b. First observations of saturopeaking: characteristics and implications. Sci. Total Environ. 573, 1615–1621.
R Core Team, 2020. R: A language and environment for statistical computing. R Foundation for Statistical Computing, Vienna, Austria.
Rocher-Ros, G., Stanley, E.H., Loken, L.C., Casson, N.J., Raymond, P.A., Liu, S.D., Amatulli, G., Sponseller, R.A., 2023. Global methane emissions from rivers and streams. Nature 621, 530–535.
Roelofs, J.G.M., Schuurkes, J.A.A.R., Smits, A.J.M., 1984. Impact of acidification and eutrophication on macrophyte communities in soft waters. II. Experimental studies. Aquatic Botany 18, 389–411.
Roley, S.S., Hall Jr., R.O., Perkins, W., Garayburu-Caruso, V.A., Stegen, J.C, 2023. Coupled primary production and respiration in a large river contrasts with smaller rivers and streams. Limnol. Oceanogr. https://doi.org/10.1002/lno.12435.
Rørslett, B., 1988. Aquatic weed problems in a hydroelectric river: The R. Otra, Norway. Regulated Rivers Res. Manage. 2, 25–37.
Rørslett, B., Johansen, S.W., 1996. Remedial measures connected with aquatic macrophytes in Norwegian regulated rivers and reservoirs. Regulated Rivers Res. Manage. 12 (4-5), 509–522.
Rørslett, B., Mjelde, M., Johansen, J., 1989. Effects of hydropower development on aquatic macrophytes in Norwegian rivers: Present state of knowledge and some case studies. Regulated Rivers Res. Manage. 3 (1-4), 19–28.
Sand-Jensen, K., 1987. In: Crawford, R.M.M. (Ed.), Plant Life in Aquatic and Amphibious Habitats. Blackwell Scientific Publications, Oxford, pp. 99–112.
Schierholz, E.L., Gulliver, J.S., Wilhelms, S.C., Henneman, H.E., 2006. Gas transfer from air diffusers. Water Res. 40 (5), 1018–1026.

Schultz, R., Dibble, E., 2012. Effects of invasive macrophytes on freshwater fish and macroinvertebrate communities: the role of invasive plant traits. Hydrobiologia 684 (1), 1–14.
Stenberg, S.K., Velle, G., Pulg, U., Skoglund, H., 2022. Acute effects of gas supersaturation on Atlantic salmon smolt in two Norwegian rivers. Hydrobiologia 849 (2), 527–538.
Stumm, W., Morgan, J.J., 1981. Aquatic Chemistry. An introduction emphasizing chemical equilibria in natural waters. Wiley Interscience, New York.
Svedang, M.U., 1992. Carbon dioxide as a factor regulating the growth dynamics of Juncus bulbosus. Aquatic Botany 42 (3), 231–240.
Thiemer, K., Immerzeel, B., Schneider, S., Sebola, K., Coetzee, J., Baldo, M., Thiebaut, G., Hilt, S., Kohler, J., Harpenslager, S.F., Vermaat, J.E., 2023. Drivers of perceived nuisance growth by aquatic plants. Environ. Manage. 71, 1024–1036.
Thiemer, K., Schneider, S.C., Demars, B.O.L., 2021. Mechanical removal of macrophytes in freshwater ecosystems: implications for ecosystem structure and function. Sci. Total Environ. 782, 146671.
Tromboni, F., Hotchkiss, E.R., Schechner, A.E., Dodds, W.K., Poulson, S.R., Chandra, S., 2022. High rates of daytime river metabolism are an underestimated component of carbon cycling. Commun. Earth Environ. 3 (1), 270.
Ulseth, A.J., Hall, R.O., Canadell, M.B., Madinger, H.L., Niayifar, A., Battin, T.J., 2019. Distinct air-water gas exchange regimes in low- and high-energy streams. Nat. Geosci. 12 (4), 259–263.
Urban, A.L., Gulliver, J.S., 2000. Comment on "Temperature effects on the oxygen transfer rate between 20 and 55 degrees C by Vogelaar, Klapwijk, Van Lier, and Rulkens. Water Res. 34 (3), 1037–1041 (2000)". Water Research 34(13), 3483-3485.
Vachon, D., Sadro, S., Bogard, M.J., Lapierre, J.F., Baulch, H.M., Rusak, J.A., Denfeld, B. A., Laas, A., Klaus, M., Karlsson, J., 2019. Paired O_2–CO_2 measurements provide emergent insights into aquatic ecosystem function. Limnol. Oceanogr. Lett. 5 (4), 287–294.
Velle, G., Skoglund, H., Barlaup, B.T., 2022. Effects of nuisance submerged vegetation on the fauna in Norwegian rivers. Hydrobiologia 849 (2), 539–556.
Verhofstad, M.J., Bakker, E.S., 2019. Classifying nuisance submerged vegetation depending on ecosystem services. Limnology 20 (1), 55–68.
Weiss, R.F., Price, B.A., 1980. Nitrous oxide solubility in water and seawater. Mar. Chem. 8 (4), 347–359.
Wetzel, R.G., Brammer, E.S., Forsberg, C., 1984. Photosynthesis of submersed macrophytes in acidified lakes. I. Carbon fluxes and recycling of CO_2 in Juncus bulbosus L. Aquatic Botany 19 (3-4), 329–342.
Wetzel, R.G., Brammer, E.S., Lindstrom, K., Forsberg, C., 1985. Photosynthesis of submersed macrophytes in acidified lakes. II. Carbon limitation and utilization of benthic CO_2 sources. Aquatic Botany 22 (2), 107–120.
Wilkinson, G.M., Cole, J.J., Pace, M.L., Johnson, R.A., Kleinhans, M.J., 2015. Physical and biological contributions to metalimnetic oxygen maxima in lakes. Limnol. Oceanogr. 60 (1), 242–251.
Wright, R.F., Couture, R.-M., Christiansen, A.B., Guerrero, J.-L., Kaste, O., Barlaup, B.T., 2017. Effects of multiple stresses hydropower, acid deposition and climate change on water chemistry and salmon populations in the River Otra, Norway. Sci. Total Environ. 574, 128–138.
Yamamoto, S., Alcauskas, J.B., Crozier, T.E., 1976. Solubility of methane in distilled water and seawater. J. Chem. Eng. Data 21 (1), 78–80.
Yang, H., Andersen, T., Dorsch, P., Tominaga, K., Thrane, J.E., Hessen, D.O., 2015. Greenhouse gas metabolism in Nordic boreal lakes. Biogeochemistry 126 (1-2), 211–225.
Zhang, J., Quay, P.D., Wilbur, D.O., 1995. Carbon isotope fractionation during gas water exchange and dissolution of CO_2. Geochim. Cosmochim. Acta 59 (1), 107–114.